Short note: various aspects of Kirchhoff migration

Th. Hertweck and Ch. Jäger

email: *Thomas.Hertweck@gpi.uka.de*
keywords: *Kirchhoff migration, topography*

ABSTRACT

In areas with topographic variations, acquisition and processing of seismic data impose a real challenge upon geophysicists. Although there exist methods to adjust the measured data to a flat datum, it is sometimes necessary or favored to migrate the data directly from topography in order to get high-quality migrated images. Kirchhoff migration is able to handle the irregular geometries and serves therefore as a suitable tool to perform such a process. However, several important things must be considered: Migration weights must refer to the actual topographic measurement surface and its local dip and need to honor the local acquisition geometry. In addition, a careful estimation of the velocity model and, thus, the traveltime tables is necessary. Then, prestack migration will not only produce correct images but also enable further studies (e. g., AVO analysis). In combination with the CRS stack (ZO and FO CRS stack, CRS stack for rugged topography) and the tomographic velocity model inversion, flexible pre- and poststack processing strategies are available.

INTRODUCTION

Migration is an important step in the processing of seismic reflection data. It should not only move reflection events to their correct spatial location but also collapse diffractions into their corresponding scattering points. While migration was often only an optional step in the early days of data processing, it is now routinely applied and has become a central part in seismic imaging. In the course of the years, migration algorithms have much improved and migrated data serve nowadays, in addition to providing a structural image, also for the estimation of macrovelocity models and as input for further analyses, e. g., amplitude versus offset (AVO) or amplitude versus angle (AVA) studies.

There exist several migration methods and a lot of implementations, 2D or 3D, time or depth, prestack or poststack (see, e. g., Yilmaz, 2001). All methods have advantages and disadvantages—a rather complete overview is given by Gray et al. (2001). Among the general methods are, for instance, finite-difference migration, reverse-time migration, or frequency-wavenumber migration. One of the oldest but still most frequently used methods is Kirchhoff migration.

The algorithmic framework of the latter has been laid by Hagedoorn (1954) who presented a graphical migration scheme based on surfaces of maximum convexity. His work was later related to the wave equation and became familiar as "Kirchhoff migration" (Schneider, 1978). The name was chosen with regard to the Kirchhoff integral which is used to describe the (forward) propagation of seismic waves within a given depth model. Since the Kirchhoff integral by itself cannot be used to solve the inverse problem, i. e., to describe backward propagation, Kirchhoff migration was introduced as its adjoint operation that describes the forward propagation of the recorded wavefield in the reverse direction. This turns out to be a very good approximation to backward propagation as long as evanescent waves can be neglected.

Kirchhoff depth migration treats each point M on a sufficiently dense grid like a diffraction point. In an a-priori given macrovelocity model, the relevant part of the Green's function of a point source at any single diffraction point M in the depth domain is calculated. The kinematic part of this Green's function is the configuration-specific diffraction-traveltime surface, also called "Huygens surface". The amplitudes of the (filtered) input seismograms are stacked along the Huygens surface and assigned to the depth point M. This explains why the Kirchhoff migration scheme is also called a "diffraction stack". If so desired, the effect of geometrical spreading can be removed from the output amplitudes by multiplying the data during the stack with a true-amplitude weight factor that is calculated from the dynamic part of the Green's function.

Kirchhoff migration has a long tradition. Although a lot of different migration algorithms have been developed in the last decades that might produce better images (at least in some scenarios), it is still a competitive and widely investigated tool. The question is: why? To answer this question, let us briefly summarize some advantages of Kirchhoff migration:

- The kinematics of the method are easy to describe. As there is a complete geometrical explanation (see, e. g., Hagedoorn, 1954), we can gain an intuitive understanding of the method itself and its pros and cons. Artifacts which might appear in limited-aperture Kirchhoff migration can also be described in a geometrical way as shown by Hertweck et al. (2001).

- There exists a firm mathematical treatment which provides the basis for Kirchhoff migration. This mathematical foundation was given by Schneider (1978) and further scientists in the following years. The theory was later extended to provide not only kinematically but also dynamically correct images of the subsurface. Bleistein (1987) was one of the first dealing with the theoretical formalism of what is today know as true-amplitude migration. Hubral et al. (1996) and Tygel et al. (1996) provided a complete unified theory to perform 3D true-amplitude seismic reflection imaging based on Kirchhoff migration and its asymptotic inverse process called demigration.

- Kirchhoff migration is able to handle laterally inhomogeneous media and provides (in a lot of cases) reliable and accurate results while being efficient at the same time.

- The method itself is very flexible and allows target-oriented processing of seismic data. Furthermore, irregular datasets and data recorded on a varying topography can easily be handled by the algorithm. The general principle allows to image dips in the subsurface that are greater than 90 degrees, i. e., it can handle turning rays—however, this is also a question of the method utilized to calculate the relevant Green's functions.

Kirchhoff migration has, of course, also some drawbacks:

- Most implementations use an asymptotic high-frequency approximation. Such an approximation causes problems for the region that is within several wavelengths of the source or receiver position, i. e., we may face problems when imaging near-surface reflectors. However, this is only a minor problem in practice and even for very shallow reflectors, Kirchhoff migration is able to produce reasonably good images.

- Multipathing may occur depending on the complexity of the macrovelocity model. Most Kirchhoff migration implementations assume that there is only one possible path from a diffraction point in the subsurface to a point at the measurement surface. There exist some extensions that can handle the multipathing problem in Kirchhoff migration, at least for a limited amount of ray paths (usually up to three). However, this comes along with a noticeable increase in computation time. The multipathing problem may also be addressed by means of Gaussian beam migration (Hill, 1990, 2001) that uses a different approach than standard Kirchhoff migration but with similar flexibility.

- Kirchhoff migration sometimes fails to image complex structures. This is closely related to the traveltime tables used in the migration process. The accuracy and the quality of the migrated image strongly depends on the method used to calculate the Greens' function. There exist a lot of methods and even more implementations to generate the traveltime tables (e. g., simple eikonal solvers or kinematic and dynamic ray tracers) which expose different speeds and accuracies. A summary and an example based on the Marmousi model is presented by Audebert et al. (1997).

- The operator aliasing problem is significant in Kirchhoff migration as we sum up discrete data along a diffraction surface without regarding the frequency content. It may happen that the steeper parts of the Huygens surface undersample the wavelet and, thus, the migrated image severely suffers from aliasing effects. Abma et al. (1999) and Biondi (2001) give a profound description of the problem and its possible solutions.

- The computational costs for the estimation of true-amplitude weights in Kirchhoff migration are, in general, high because several dynamic ray quantities are involved that must be computed in addition to the traveltime itself. However, there exist some approaches to overcome this problem: they are either based on simple approximations of the complete true-amplitude weight factor (Peres et al., 2001) or on the determination of the weight function from traveltimes only (Vanelle and Gajewski, 2002).

As shown by Gray (1998), most migration methods are accurate when imaging regions of typical structural complexity. The differences are usually less than the uncertainty in estimating the velocity model. Therefore, using much more expensive tools to increase the accuracy by a small factor is not justified from an economical point of view. Because of its accuracy and relative cheapness, Kirchhoff migration is a workhorse in seismic data processing, especially for handling data measured on a surface with topographic variations or irregularities.

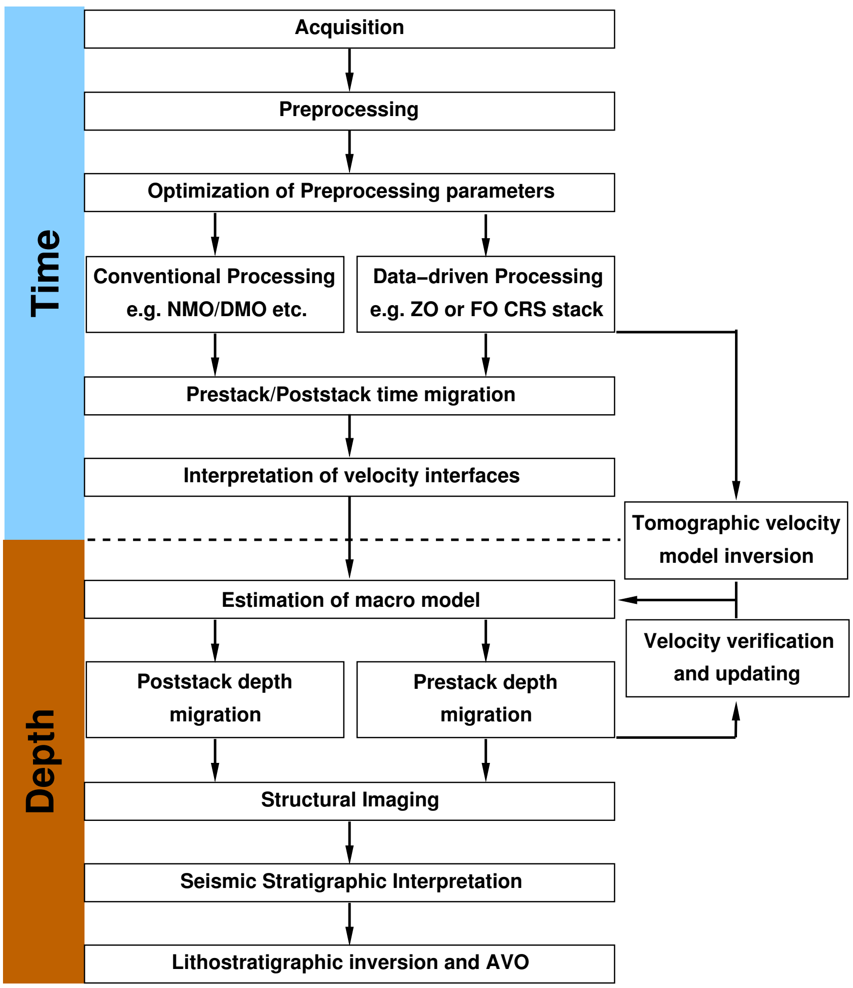

Figure 1: Seismic data processing flowchart. The different steps are usually carried out by different groups, e. g., contractors, oil company processing groups, interpretation departments, or quality control teams [after Farmer et al. (1993)].

Strategies at Karlsruhe University

All data examples shown in the following section were processed with `Uni3D`, a Kirchhoff true-amplitude migration program developed at Karlsruhe University and presented in an article by Jäger and Hertweck in this issue. Together with the ZO and FO CRS stack programs (see, e. g., Bergler et al. in this issue) and the tomographic velocity model inversion method based on CRS stack attributes (see Duveneck et al. in this issue), there exist flexible pre- and poststack processing strategies. A general overview of processing steps is given in the flowchart (Figure 1).

In order to test all our algorithms, synthetic earth models as well as pre- and poststack datasets are created. CRS stack results may be easily compared to the forward-modeled seismograms. The velocity model obtained by tomographic inversion by means of CRS stack attributes can be compared to the original earth model. Both, the CRS stack results and the estimated (or true) velocity model, enter into the depth migration which should then be able to recover a correct image of the subsurface, either by pre- or poststack migration. We are, thus, able to perform some of the main steps of seismic data processing in a controlled environment that allows to check the results and our software. Real data impose, of course, many more challenges upon geophysicists and software developers compared to synthetic data examples—however, results cannot be checked and we need to know in advance about the pros and cons and the reliability of our algorithms. In the next section, special aspects of the migration process and various data examples are presented.

SPECIAL ASPECTS AND DATA EXAMPLES

One can find a lot of papers about different migration methods and various aspects concerning accuracy, speed, or flexibility—however, one usually underestimates the important but fundamental problem of finding the correct velocity model for migration. Developing extremely accurate migration algorithms makes only sense if we are able to estimate the correct seismic velocities for migration. Duveneck (see his article in this issue) presents a new way of estimating an initial macrovelocity model utilizing tomographic inversion based on CRS stack attributes. In combination with the CRS stack itself, prestack (depth) migration and, afterwards, the update of the velocity model, we might find the correct velocity model with only view iterations.

To test our processing tools, a synthetic prestack dataset was created by means of dynamic ray tracing for the model shown in Figure 3(a). The dataset consists of 60,000 traces: 600 shots ranging from -2000 m to 9980 m at $z = 0$, and each shot with 100 receivers (offset range from 0 up to 1980 m). The time sampling is 4 ms, shot and receiver increments are 20 m. Noise was added in order to make the synthetic dataset more realistic. This dataset entered into the ZO CRS stack that produced a ZO section with 1201 traces and a trace increment of 10 m. The result is shown in Figure 2(b) and compared to a forward-modeled ZO section with the same noise level as the prestack dataset (Figure 2(a)). It can clearly be seen that the CRS stack produced a kinematically correct image almost without noise.

In addition, several kinematic wavefield attributes (wavefront curvatures, normal ray emergence angles) associated with each simulated zero-offset sample came out of the ZO CRS stack process. They entered into the tomographic velocity model inversion (see the article by Duveneck in this issue) that produced the smooth, laterally inhomogeneous, isotropic velocity model shown in Figure 3(b). This inverted velocity model as well as the true velocity model shown in Figure 3(a) were used in the depth migration examples.

Poststack migration Figure 4 shows the results of poststack depth migration of the CRS stacked section using the true (Figure 4(a)) and the inverted (Figure 4(b)) velocity model. Artifacts are mainly caused by holes and missing diffraction events in the input seismograms—this is an effect of the ray tracing program used to generate the input prestack data. The SEP eikonal solver was utilized to create the traveltime tables. The target zone ranges from $x = -1500$ m to $x = 8000$ m and $z = 200$ m to $z = 3700$ m. The increments in the depth migrated images are $dx = 10$ m and $dz = 5$ m. The migration result obtained with the inverted velocity model looks quite similar to the one obtained with the true velocity model.

Prestack migration Further studies of the velocity model are possible when checking the image gathers after prestack migration. Figure 5 shows the results of prestack depth migration using the true (Figure 5(a))

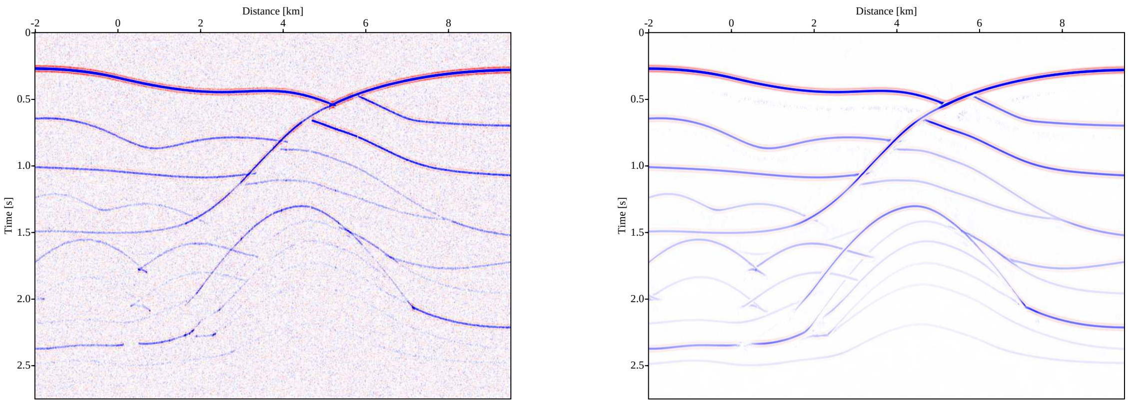

(a) Forward-modeled ZO section

(b) CRS-simulated ZO section

Figure 2: Zero-offset sections a) forward modeled by dynamic ray tracing (without diffraction events) and b) simulated by means of the ZO CRS stack from noisy prestack data.

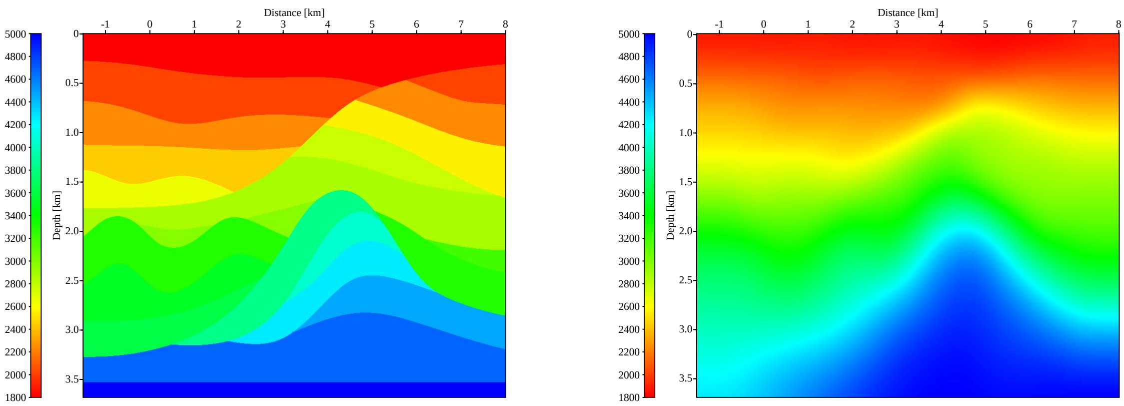

(a) True velocity model in m/s

(b) Inverted velocity model in m/s

Figure 3: a) part of the true blocky velocity model corresponding to the inversion target zone; b) smooth velocity model estimated by means of tomographic inversion using CRS stack attributes. Colors denote P-wave velocities in m/s.

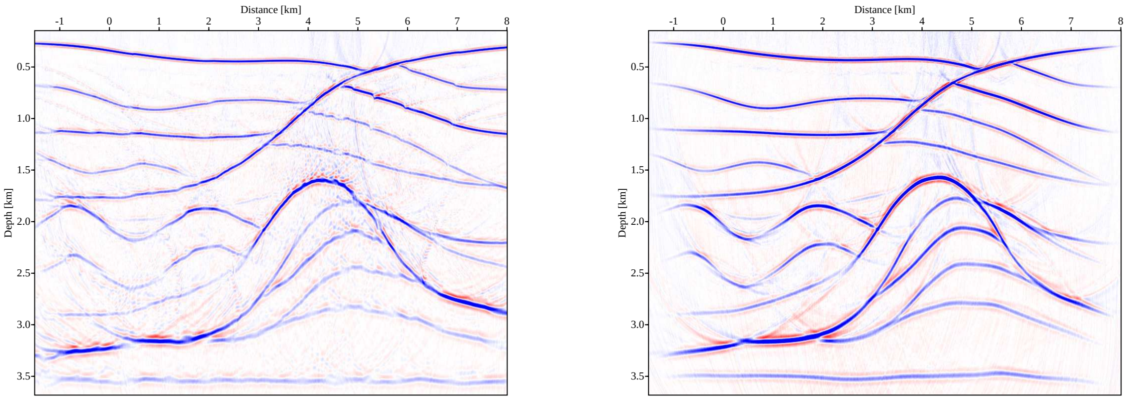

(a) Migration with true velocity model **(b)** Migration with inverted velocity model

Figure 4: Poststack migration from flat measurement surface using a) the true velocity model, and b) the velocity model based on tomographic inversion. Artifacts are mainly caused by holes and missing diffraction events in the input seismograms—this is an effect of the ray tracing program used to generate the input prestack dataset.

and the inverted (Figure 5(b)) velocity model. Artifacts are mainly caused by holes and missing diffraction events in the input seismograms—this is an effect of the ray tracing program used to generate the input prestack dataset. The SEP eikonal solver was utilized to create the traveltime tables. The target zone ranges from $x = 0$ m to $x = 8000$ m and $z = 200$ m to $z = 3700$ m. The increments in the depth migrated images are $dx = 20$ m and $dz = 10$ m. All offsets up to 1000 m were stacked in order to produce the pictures. The deeper reflectors would improve if all available offsets up to 2000 m were stacked—however, this procedure (without muting) would result in a distorted image for shallow reflectors due to the pulse stretch observed in the image gather (Figure 6).

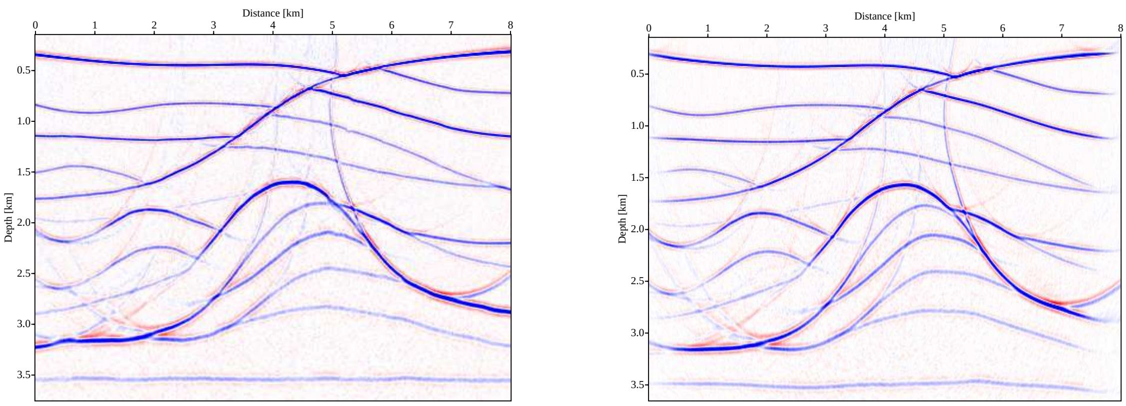

(a) Migration with true velocity model **(b)** Migration with inverted velocity model

Figure 5: Prestack depth migration for data measured at $z = 0$ using a) the true velocity model, and b) the inverted velocity model. All offsets up to 1000 m were stacked after the migration process. The migration artifacts are mainly caused by the missing diffraction events in the input dataset.

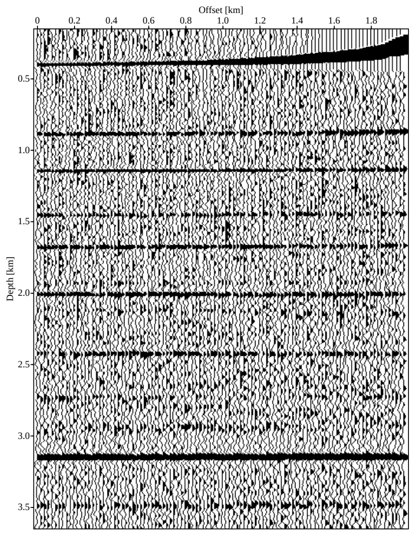

(a) Location $x = 1200\,\mathrm{m}$

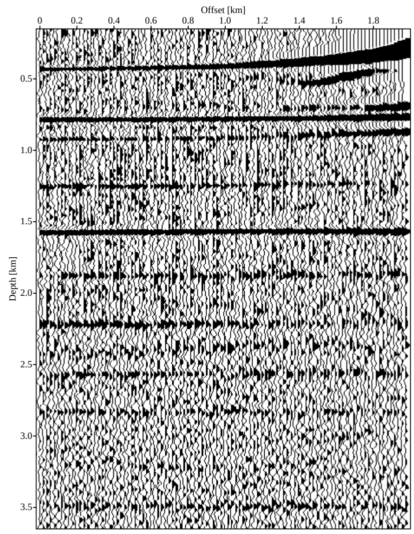

(b) Location $x = 4200\,\mathrm{m}$

Figure 6: Image gather at a) $x = 1200\,\mathrm{m}$ and b) $x = 4200\,\mathrm{m}$ from the prestack depth-migrated image using the inverted velocity model, see Figure 5(b). Most events are perfectly flat.

Most events in the image gathers are flat, i. e., the inverted smooth velocity model is a good approximation of the true velocity model. If such a model is used as a starting model in prestack migration, the best detailed model can be found with only few iterations.

Migration from topography These examples are, of course, idealized compared to real data. The problems of crooked lines, topographic variations and irregular acquisition geometries have not been addressed so far. To study some of these problems, a new prestack dataset was created for the model shown in Figure 3(a). However, the data was not simulated along the surface $z = 0\,\mathrm{m}$ but shots and receivers were placed along a surface with topographic variations. The actual topography is shown in Figure 7(a), the modeled zero-offset section in Figure 7(b). The prestack dataset is not shown here—it has the same acquisition parameters as the prestack dataset measured at $z = 0\,\mathrm{m}$.

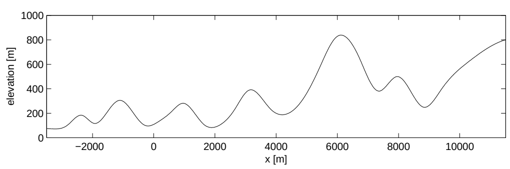

(a) Topography

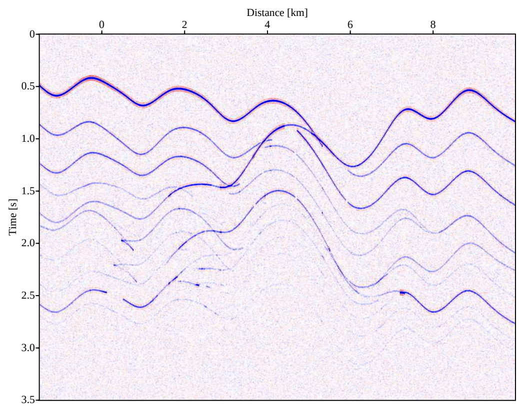

(b) Forward-modeled ZO section

Figure 7: a) topography of the measurement surface; b) zero-offset section forward modeled by dynamic ray tracing (without diffraction events) on the measurement surface with topographic variations.

Figure 8 shows the result of prestack depth migration directly from topography. As before, artifacts are mainly caused by holes and missing diffraction events in the input seismograms. The SEP eikonal solver was utilized to create the traveltime tables. The target zone ranges from $x = -2000$ m to $x = 10000$ m and $z = 200$ m to $z = 3700$ m. The increments in the depth migrated images are $dx = 20$ m and $dz = 10$ m. All offsets up to 1500 m were stacked in order to obtain this picture. The deepest reflector is flat and correctly imaged, i. e., the handling of the topography in the migration itself and the creation of the traveltime tables was successful.

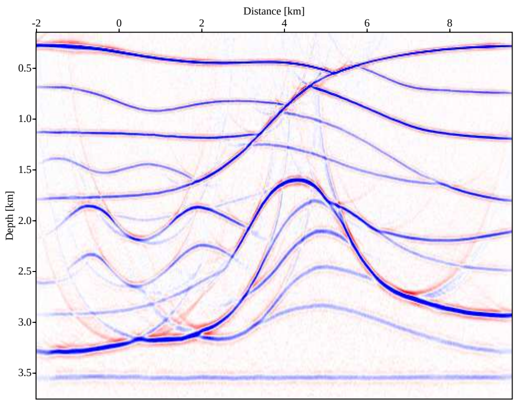

Figure 8: Prestack depth migration directly from topography. Offsets up to 1500 m were stacked after the migration process. The deep reflector is correctly imaged.

Amplitude comparison True-amplitude migration should be able to recover the correct reflection coefficients for reflectors in the migrated image, at least if we neglect transmission effects and other effects on the amplitude. When working with topography, the question now is whether it is better to fix the distance between receiver groups to be equally spaced along the topographic surface or along the horizontal axis. If we fix them along the topography by Δg, then the horizontal increment $\Delta\xi$ will be irregular but always less or equal to Δg. For this reason, the depth migrated images will in general have less aliased noise (Gray et al., 1999). To study the effect of irregularities, we created an irregular ZO section with 1006 traces for the model shown in Figure 3(a). The trace increments randomly vary between 9 m and 15 m with an average increment of 11.9 m. This section was true-amplitude depth migrated using the true velocity model; afterwards, the amplitude along the first reflector at a depth of about $z = 400$ m was picked. Figure 9(a) shows the theoretical values and picked amplitudes for two specific cases: a) migration was performed with an average (constant) trace spacing; it can clearly be observed that the overall amplitude behavior is correct. However, fluctuations occur which make further analyses difficult. The same holds for reflector amplitudes after true-amplitude prestack depth migration and might, thus, affect AVO or AVA studies. b) migration was performed considering the actual local trace increments in the true-amplitude weight function. This approach allows an almost perfect reconstruction of the true reflection coefficients. When working with topographic variations and irregular acquisition geometries, it is essential to honor the local trace increments and topographic variations in order to get the best possible migration result.

CONCLUSIONS

Although established for a long time, the use of classical Kirchhoff migration is still justified and it constitutes a workhorse in seismic data processing. Some of its main advantages and drawbacks were presented in this paper. Especially when working with large datasets irregularly measured along surfaces with topographic variations, the target-oriented Kirchhoff migration approach shows its productive efficiency. In combination with our time-processing tools such as ZO and FO CRS stack (which, in future, are also available for datasets with topographic variations) and the program to estimate the velocity model based on tomographic inversion, we have flexible software solutions for the main processing steps in seismic reflection data handling.

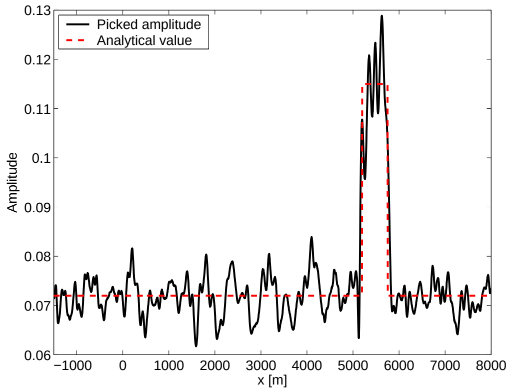

(a) Constant average trace spacing

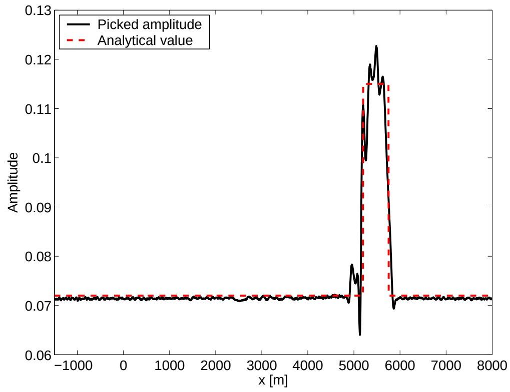

(b) Local trace spacing

Figure 9: Amplitude comparison for the first reflector after true-amplitude migration using a) an average constant trace spacing and b) the local trace spacing in the weight function. The latter allows to reconstruct the true reflection coefficient almost perfectly.

ACKNOWLEDGMENTS

This work was kindly supported by the sponsors of the *Wave Inversion Technology (WIT) Consortium*, Karlsruhe, Germany. We thank Eric Duveneck and Jürgen Mann for their help and the fruitful discussions.

REFERENCES

Abma, R., Sun, J., and Bernitsas, N. (1999). Antialiasing methods in Kirchhoff migration. *Geophysics*, 64(6):1783–1792.

Audebert, F., Nichols, D., Rekdal, T., Biondi, B., Lumley, D., and Urdaneta, H. (1997). Imaging complex geologic structure with single-arrival Kirchhoff prestack depth migration. *Geophysics*, 62(5):1533–1543.

Biondi, B. (2001). Kirchhoff imaging beyond aliasing. *Geophysics*, 66(2):654–666.

Bleistein, N. (1987). On the imaging of reflectors in the earth. *Geophysics*, 52(7):931–942.

Farmer, P., Gray, S., Hodgkiss, G., Pieprzak, A., Ratcliff, D., and Whitcombe, D. (1993). Structural Imaging: Toward a Sharper Subsurface View. *Oilfield Review*, 5(1):28–41.

Gray, S. (1998). Speed and accuracy of seismic migration methods. Mathematical Geophysics Summer School (Proceedings), Stanford University, USA. http://sepwww.stanford.edu/etc/sam_gray/.

Gray, S., Etgen, J., Dellinger, J., and Whitmore, D. (2001). Seismic migration problems and solutions. *Geophysics*, 66(5):1622–1640.

Gray, S., MacLean, G., and Marfurt, K. (1999). Crooked line, rough topography: Advancing towards the correct seismic image. *Geophysical Prospecting*, 47(5):721–733.

Hagedoorn, J. (1954). A process of seismic reflection interpretation. *Geophys. Prosp.*, 2(2):85–127.

Hertweck, T., Jäger, C., Goertz, A., and Schleicher, J. (2001). Aperture effects in 2.5-D Kirchhoff migration. Submitted to Geophysics; partly published in Annual WIT Report 2001.

Hill, N. (1990). Gaussian beam migration. *Geophysics*, 55(11):1416–1428.

Hill, N. (2001). Prestack Gaussian-beam depth migration. *Geophysics*, 66(4):1240–1250.

Hubral, P., Schleicher, J., and Tygel, M. (1996). A unified approach to 3-D seismic reflection imaging, Part I: Basic concepts. *Geophysics*, 61(3):742–758.

Peres, O., Kosloff, D., Koren, Z., and Tygel, M. (2001). A practical approach to true-amplitude migration. *J. Seis. Expl.*, 10:183–204.

Schneider, W. (1978). Integral formulation for migration in two and three dimensions. *Geophysics*, 43(1):49–76.

Tygel, M., Schleicher, J., and Hubral, P. (1996). A unified approach to 3-D seismic reflection imaging, Part II: Theory. *Geophysics*, 61(3):759–775.

Vanelle, C. and Gajewski, D. (2002). True-amplitude migration weights from traveltimes. *Pure and Applied Geophysics*, 159:1583–1599.

Yilmaz, Ö. (2001). *Seismic Data Analysis*. Soc. Expl. Geophys., Tulsa.